Simulation of an Under Lake Infrastructure for Capture and Storage of Solar Energy (ULISSE)

D. Bello-Mendes[1], R. Rozsnyo[1], W. van Sprolant[2]
[1]hepia, HES-SO, Geneva, Switzerland
[2]CvS Énergies sàrl, Geneva, Switzerland

Abstract

In this paper we present a Comsol Multiphysics simulation model of a reduced size ULISSE mock-up. The mock-up is immersed in a container, playing the role of the lake. Both are filled with water at the room temperature. Then starts a cycle imitating the change of seasons. Hot water at 33.5 ^{0}C is injected by a pump in the ULISSE mock-up chasing the initial water. After a period of rest, the water is pumped back. The recovered energy is calculated. Real-time measurements are made by temperature sensors and water flow sensors allowing comparisons with the simulation results.

Keywords: Renewable Energies, Lacustrine Thermal Energy, Energy Storage, Multiphysics Simulation

Introduction

The transition from fossil fuels to renewable energies requires finding new sources of energy. It turns out that the hydrothermal potential of the lakes would cover a significant part of these renewable energy needs [1],[2],[3]. The existing Thermal Lacustrine Networks (TLNs) are efficient in summer allowing the building air conditioning by « free-cooling » (without heat pumps) thanks to the cold water pumped from the bottom of the lakes. However, in winter, the heating of the buildings is 4 to 5 times less efficient due the use of heat pumps and because of the lower temperature differential of the water round-trip of the lakes. The ULISSE project, supported by the Swiss Federal Office of Energy, aims to build an underwater tank made of a semi-rigid envelope that could be filled with the warm water pumped from the surface of the lakes, heated by the sun during the hot season and to keep that water as warm as possible thanks to the thermal insulation properties of the envelope until the cold season [3]. In winter, that water would be pumped back from the tank. The higher temperature (versus normally at the lake bottom) of the pumped water increases its energy density (MJ/m^3) which would allow to reduce by 95% the hydraulic pumping energy and up to twice the Carnot efficiency for the heat pumps of the said TLNs (Fig. 1). This concept reproduced over the fifteen largest lakes in Switzerland would allow to economize 3 TWh of electricity consumption during the winter [3].

Experimental Set Up

The ULISSE tank immersed under a lake is a huge construction challenging many fields of engineering. Before trying to build such a tank, it made sense to prove the concept over a reduced size mock-up and to study the ability of the system to store the solar energy (Fig. 2). The experimental model makes it possible to reproduce the different operating phases of the ULISSE tank to analyze and establish the efficiency of its sub-lacustrine seasonal energy-heat

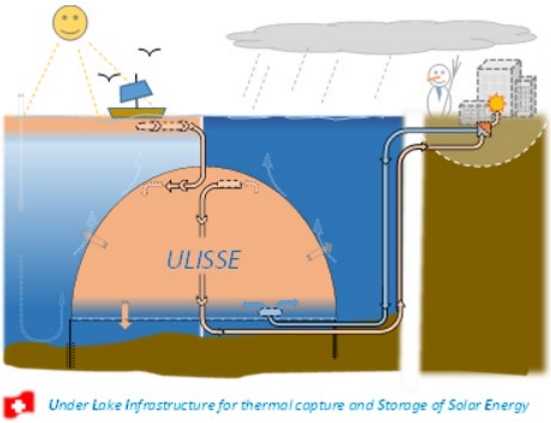

Figure 1. Illustration of the ULISSE principle.

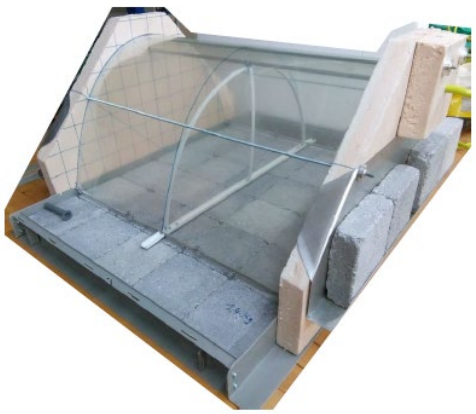

Figure 2. The reduced size ULISSE mock-up.

storage capacity. The autumn stagnation phase is used to establish the stagnation heat loss and the cooling time constant characteristic. In addition, the experimental model also makes it possible to reproduce and measure the heat exchange flows, during the « dynamic » phases, of summer loading of temperate water and winter unloading. The test model (Fig. 2) has a reduced scale of 1/806 over the length and 1/166 over the radius. At the two longitudinal ends, the envelope is « strongly insulated » (pseudo athermal walls) by a 4 cm thick extruded polystyrene plate. The hyperbolic envelope of the mock-up is reduced to a thin (2 mm) and transparent sheet of polycarbonate. This sheet (62 x 90 cm = 5'580 cm^2) is curved in its large dimension (90 cm) and is fixed at the base between two threaded stainless steel rods spaced 57 cm apart and a third located at the top. Two other threaded rods are still placed halfway up. These threaded rods are used to hold the enclosure between the two end insulating plates. The resulting curvature being close to the hyperbola with an average radius of 30 cm. The corresponding volume of the mock-up is 77 liters.

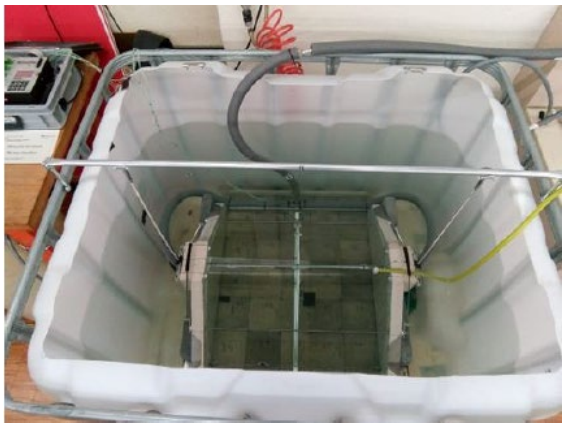

Figure 3. The reduced size ULISSE mock-up immersed in a container.

As a first approximation, this makes it possible to neglect the longitudinal heat loss of the experimental model and to highlight the predominance of the transverse heat loss of the envelope, including that by the lake bottom as well as the free convection which tends to reduce the internal stratification, leading to energetic losses.

The mock-up is placed in a plastic IBC container with a 1'000 liter frame (Fig. 3), fixed on a plastic pallet (120 x 100 cm). The ratio between the volume of water in the tank and the mock-up is a maximum of 12. For the introduction of the mock-up, a rectangular opening (100 x 80 cm) is made at the top of the tank. The mock-up is maintained on the bottom of the container (against the Archimedes thrust of the PSX end plates), by a ballast made of 4 stainless steel flats (10 kg gross recovery) and by the support of two adjustable retaining rods from the tank structure. The lower opening of the mock-up is placed on two layers of concrete pavers (total thickness 8 cm) reproducing the conductivity and the thermal capacity of the lake bottom.
The temperature of the water in a real ULISSE type reservoir is a priori around 20°C while that at the bottom of the lake is 5°C, i.e. a difference of 15°C. The experiments on the mock-up are made with a supply from the domestic hot water and cold water network. The temperature is regulated by a conventional shower mixer and an intermediate thermal stabilization tank (Fig. 4). For example, with a temperature difference of 15°C and considering the ratio between the volumes of water between the mock-up and the container, the temperature of the container can gradually increase by about 1°C if it is insulated and not cooled.

Figure 4. The water thermo-regulation system.

Measurements

The mock-up is equipped in its upper part with a ramp for injection and extraction of temperate water to reproduce the summer loading and the winter unloading of energy in the form of heat (Fig.5).

Figure 5. The injection-extraction ramp.

The temperature and water flow measurements at the level of the ramp make it possible to quantify the heat-energy introduced and extracted from the mock-up over a complete cycle (pseudo-annual). The measurements are mainly thermal in order to know the temperature and also to indirectly deduce the convective movements of water in the mock-up as well as those in the container representing the lake. The temperature probes (Fig. 6) are type K thermocouples and are placed in the mock-up on a transverse PVC support which can be moved longitudinally as well as on the upper water

distribution/extraction ramp. Nine thermocouples are placed, in pairs, at different heights on the transverse support; one on the central axis and the other on the side edge of the support as well as two laterally (in position or opposite end) on the summit ramp (Fig. 7, 11). As shown by Figure 2, the support is placed in the transverse symmetry plane of the mock-up. The thermocouples are connected to a micro logger measurement and data acquisition interface (CR3000 from Campbell Scientific). The latter also records the flow rate/volume of loading and unloading hot water from the mock-up, via the pulse flow meter located on the hydrothermal supply plate.

Figure 6. Type K thermocouples.

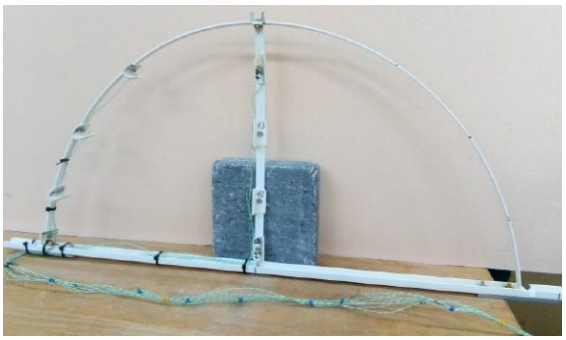

Figure 7. The cross support of thermocouples.

Governing Equations

Fluid flow modelling

We assume the water flow in the system laminar and incompressible. The flow is due to the natural convection and the injected water. Thus, the equations governing the flow are the Navier-Stokes equations without taking into account the viscosity of the water. The momentum conservation is given by Eq. 1:

$$\rho_w \frac{\partial \boldsymbol{u}}{\partial t} + \rho_w(\boldsymbol{u}\cdot\nabla)\boldsymbol{u} = -\nabla p + \rho_w \boldsymbol{g}, \qquad (1)$$

where, $\boldsymbol{u}$ is the velocity field, $\boldsymbol{g}$ the gravity field, ρ_w the water density and p the pressure scalar field. This equation must be completed by the equation of the mass conservation, Eq. 2:

$$\nabla\cdot\boldsymbol{u} = 0. \qquad (2)$$

However, to take into account the effects of the gravity field, we used the Boussinesq approximation on the density [4]:

$$\rho_w = \rho_{ref}\big(1-\alpha_p\big)\big(T-T_{ref}\big), \qquad (3)$$

where ρ_{ref} is the reference density of the water, i.e. at the reference temperature, $T_{ref} = 20$ °C, and α_p is the dilatation coefficient at constant pressure at the reference temperature given by Eq. 4:

$$\alpha_p = -\frac{1}{\rho_w}\left(\frac{\partial \rho_w}{\partial T}\right)_p. \qquad (4)$$

Eq. 1 and Eq. 2 must be completed by the boundary and the initial conditions. The boundary conditions are on the walls (interior and exterior) $\boldsymbol{u} = \boldsymbol{0}$ and on the free surface $p = p_{ref}$ where p_{ref} is the atmospheric pressure. At the initial conditions, corresponding to $t = 0$, the water has a velocity field $\boldsymbol{u} = \boldsymbol{0}$. The pressure field given by the relation $p = p_{ref} + \rho_w \boldsymbol{g}\cdot(\boldsymbol{r}-\boldsymbol{r_{ref}})$ corresponding to the fundamental law of the hydrostatics.

Heat transfer in solids and fluids modelling

The heat transfer in all media is governed by Eq. 5:

$$\rho C_p \frac{\partial T}{\partial t} + \rho C_p \boldsymbol{u}\cdot\nabla T - \nabla\cdot(-k\nabla T) = 0, \qquad (5)$$

where, ρ is the density of a given medium, C_p its heat capacity at constant pressure and k its thermal conductivity. The bidirectional coupling between Eq. 1 and Eq. 5 is made through the convective term $\rho C_p \boldsymbol{u}\cdot\nabla T$ and the Boussinesq approximation. Eq. 5 must be completed by boundary and initial conditions. At $t = 0$, the system was in thermal equilibrium with the exterior. Thus, the initial temperature,T_0, is given by the exterior temperature, $T_0 = T_{ext} = 21.3$°C. The boundaries of the water injection holes are set to the temperature $T_i = 33.5$°C during the phase of injection and to thermal insulation during the other phases. All the other boundaries are set to a convective heat flux boundary condition. The convection coefficient, h, was set to the value $h = 11\ W\cdot m^{-1}\cdot K^{-1}$.

In general, the process having three phases, the initial conditions for a given phase is the last state of the system in the previous one.

Modelling with Comsol Multiphysics

The geometry of the system has two plane symmetries. For the sake of simplicity, we didn't represent details such as screws, nuts, probe holders and the walls of the container. Thus, the simulation domain is the water with the immerged mock-up. A quarter of the system, shown by Figure 8, has been modelled. The height of the system is the initial water height in the container.
The Laminar Flow interface of the CFD Module and the Heat Transfer in Solids and Fluid interface of the Heat Transfer Module were used. The Nonisothermal Flow interface ensured the multiphysics coupling between the fluid flow and the heat transfer. The Boussinesq approximation was selected for that coupling.

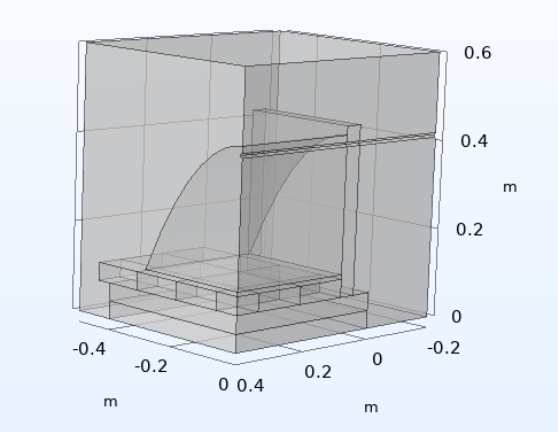

Figure 8. The geometrical representation in Comsol.

In order to complete the governing equations and the boundary conditions described in the previous section, two symmetry conditions were added at the symmetry planes locations as boundary conditions due to the geometrical representation.
The simulation was done with the default time dependent solver. The whole cycle consists in three studies corresponding to three phases summarized in Table 1.

Phase	Description	Time Range (min)
1	Water injection	[0;64]
2	Relaxation	[64;70]
3	Water extraction	[70;134]

Table 1: The three phases

During the phase 1, the water in the mock-up at ambient temperature is flushed by the injected water from the injection ramp. Then follows a period of relaxation, phase 2, where the water in the tank is cooled due to diffusion and convection. In the phase 3, the water is pumped out from the mock-up. The question to be answered is how much energy can be recovered from the amount that what was stored in the phase 1. The volume of the water in the container is changing during the injection and pumping phases. The injected volume in the mock-up is about 140 liters (approximately twice the real mock-up volume, its lower part being open), corresponding to an increase of the water height in the container about 12 cm. We assumed that this height change had a low impact on the temperature evolution inside the mock-up. Thus, in order to spare computation time, we didn't model the volume evolution of the container (by a deformed mesh or a diphasic air-water flow technique). We simply set an Outflow condition at the free surface boundary, activating the Back Flow Suppression during the phases 1 and 2 and disabling it during the phase 3. The Normal Flow option and the Compensation for Hydrostatic Pressure remained always activated at the open boundary. The mock-up hyperbolic boundary (Fig. 9), was defined as an Interior Wall. Its material properties were defined as a Single Layer Material.

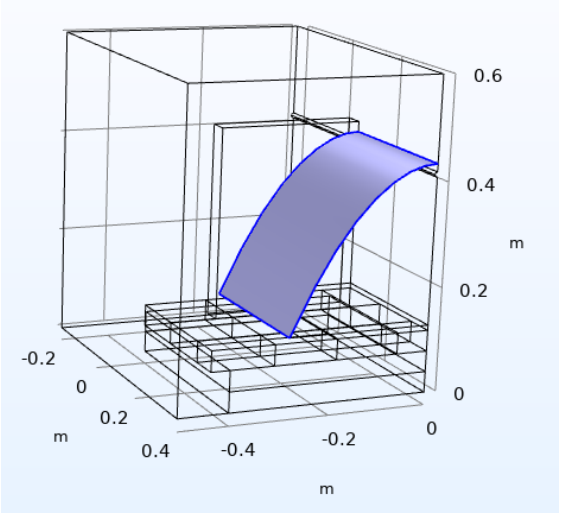

Figure 9. The mock-up hyperbolic boundary.

The boundaries of the injection ramp (Fig. 10) from where injection or pumping occurs were set the boundary conditions given by the Table 2 where the velocity of the injection is $v_0 = 0.3096\ m \cdot s^{-1}$. The

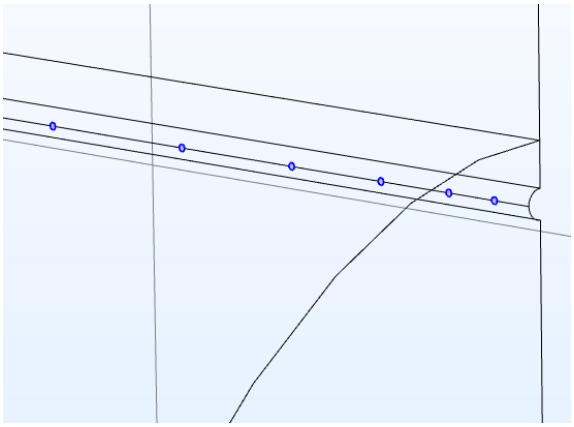

Figure 10. The water injection and pumping boundaries.

area of the surface of injection of a hole being equal to $S = 4.9159 \cdot 10^{-6}\ m^2$, the corresponding water debt per hole is $0.0913\ l \cdot min^{-1}$ which is about $2.19\ l \cdot min^{-1}$ for the total injection debt. The injection velocity was ramped in order to get numerical stability.

Phase	Laminar Flow	Heat Transfer
1	v_0 (ramped)	T_i
2	No Slip	Thermal Insulation
3	$-v_0$ (ramped)	Thermal Insulation

Table 2: Boundary conditions for injection boundaries at the different phases.

Simulation Results, Comparison with Experimental Measurements.

We used for comparisons between simulation and experimental measurements the temperature evolution at the location of the probes shown by Figure 11 during a full cycle: injection, relaxation, extraction.

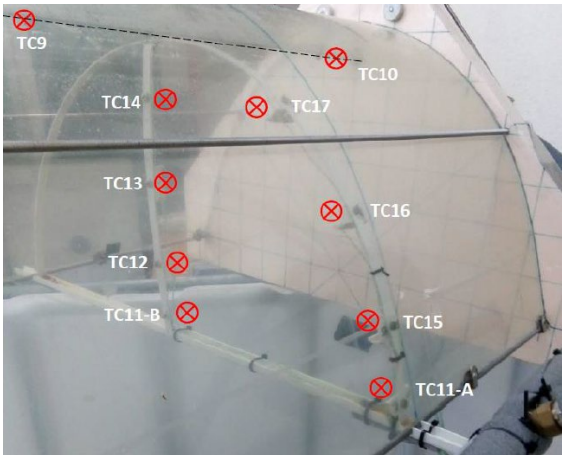

Figure 11. Probes position for comparisons between simulation results and measurements.

The experimental results are shown by Figure 12.

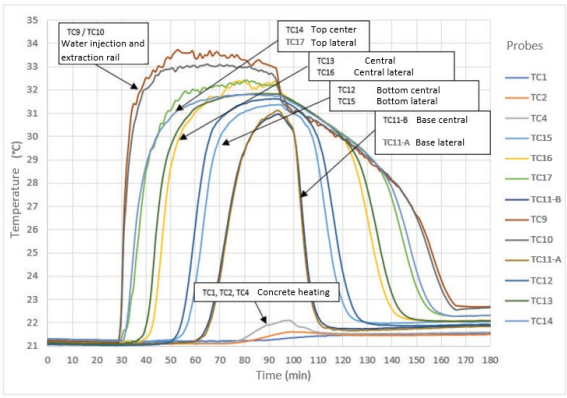

Figure 12. Temperature evolution measured by probes during a full cycle.

The probes were also placed in the Comsol model at the same locations. The temperature evolution obtained by simulation is shown by Figure 13.

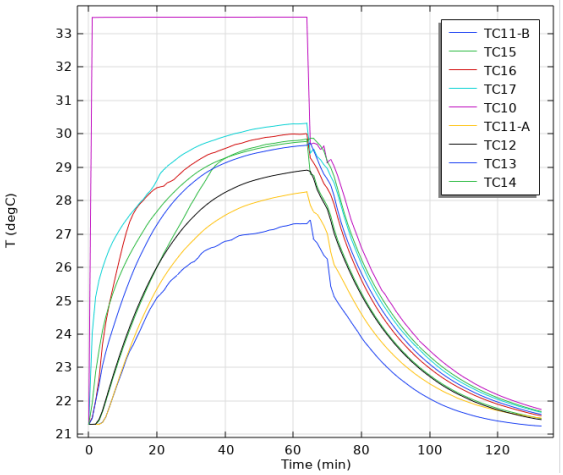

Figure 13. Temperature evolution obtained by simulation during a full cycle.

Figure 14 shows the temperature distribution at the end of water injection. We may notice that the tank is filled with warm water between approximatively 27 °C and 33.5 °C.

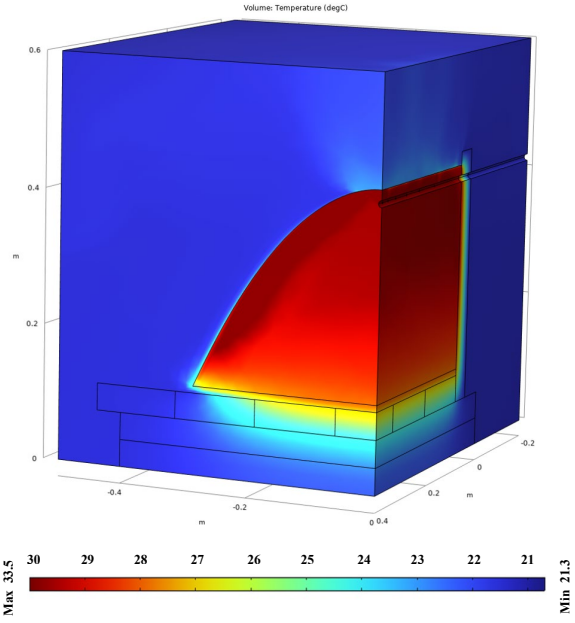

Figure 14. Temperature distribution in °C at t = 64 min at the end of the water injection.

Figure 15 shows the velocity distribution at the end of the water injection. We may notice the existence of convection currents surrounding the mock-up and on the top of the insulating shell. These currents are responsible of the energy dissipation by convection. Figure 16 shows the temperature distribution while extracting the water. The gradient of the temperature distribution reveals that the energy is also dissipated by diffusion from the mock-up to the bottom of the system.

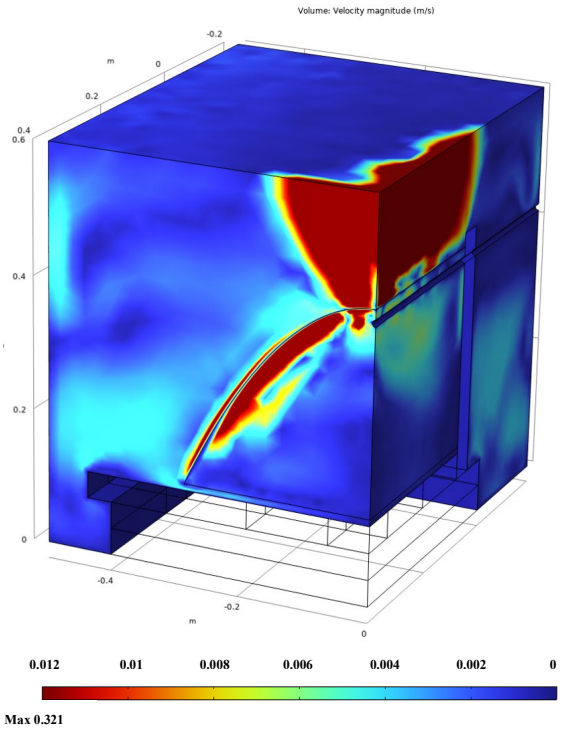

Figure 15. Velocity magnitude distribution in $m \cdot s^{-1}$ *at* t *= 64 min at the end of the water injection showing the convection currents. The maximum is 0.321* $m \cdot s^{-1}$ *at the injection inlet.*

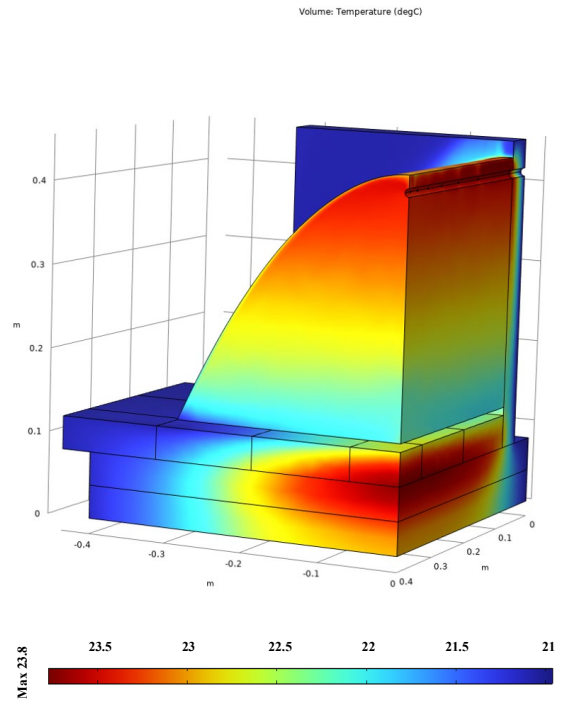

Figure 16. Temperature distribution in °C *at t = 89 min during the water extraction.*

Comparing the temperature response by simulation to the temperature response by experiments, we may notice the same global behavior and that the reached temperatures are coherent. The simulation curves look like the voltage curve response of a charge and discharge of an electric capacitor, except in the relaxation phase (6 min of duration) where the inflexion of the response curve is inverted. In the experimental curves this inverted inflexion lasts longer and we have a much more important response delay between the probes.

In order to explain the differences, we must bear in mind the simplification made in the geometry of our simulation model. For instance, the support of the probes has not been modeled. The probes are screwed on the support and probably there is a perturbation of the measures due to heat absorption by the support elements and the probes themselves. The probes also have an uncertainty of ± 1.5°C in the range of working temperatures according to the manufacturer's specifications. Their location, in the experiment versus in the simulation model, has also an uncertainty that was difficult to be quantified and that might be a sensitive factor. We may also notice that the injection temperature in the experiments is not homogeneous in the injection ramp, oscillating between 33°C and 33.8°C, whereas in the simulation model it's constant equal to 33.5°C. Thus, the evolution of temperatures shown by the simulation can be considered close to the reality even if we don't have exactly the same curve shapes. However, that point has still to be investigated.

The qualitative behavior of the system is pretty well reproduced by the simulation which helps to understand how the convection currents move away the thermal energy stored in the mock-up from its bottom open boundary, evacuating heat along its exterior boundaries to the container open boundary above the top of the mock-up (Fig. 15). An amount of the thermal energy is also absorbed by diffusion in the concrete ground of the system. While pumping out the warm water, we may observe the gradient of temperature distribution, the colder water replacing the warmer water from the bottom to the top, where occurs pumping out.

Our target being the quantification of the recovered energy after storage [5], we analyzed in the postprocessing the energy balance during the cycle. The theoretical amount of internal energy, U_0, stored in the mock-up of volume, V_m, at $t = 0\ min$ is:

$$U_0 = \rho_w(T_0) V_m C_p(T_0)\left(T_0 - T_{ref}\right). \qquad (6)$$

The theoretical amount of internal energy, U_i, injected into the mock-up during 64 min is:

$$U_i = 24\rho_w(T_i) v_0 S \Delta t C_p(T_i)\left(T_i - T_{ref}\right), \qquad (7)$$

where S is the area of the surface of injection of each of the 24 injection holes and Δt is the duration of the injection in seconds. The injected water is assumed to have a constant temperature. The internal energy of the tank at any time may also be calculated directly by Comsol Multiphysics: the internal energy of a domain at a given temperature distribution is the energy necessary to increase the temperature of the system from the reference temperature, T_{ref}, to that

temperature distribution. Formula (7) may also be implemented in Comsol. If U_{64} is the internal energy at the end of injection, we expect to have the relation $U_{64} < U_0 + U_i$ because, during the injection, a part of the energy in the mock-up is lost through convection and diffusion. Thus, the stored energy, E_S, is given by the difference $E_s = U_{64} - U_0$. If U_{70} is the internal energy of the mock-up at the end of the relaxation phase, corresponding to time t_{70}, the stored energy available for extraction, E_a, is given by $E_a = U_{70} - U_0$. The energy loss, E_L, during relaxation is $E_L = U_{64} - U_{70}$. The internal energy of the extracted water, U_x, was computed with Comsol Multiphysics by using a probe giving the average surface temperature at the time t, $\bar{T}_k$, on the extraction surface of each of the 6 holes of the simulation model and time integration over the phase 3 ending at time t_{134}:

$$U_x = 4v_0 S \sum_{k=1}^{6} U_k \tag{8}$$

where,

$$U_k = \int_{t_{70}}^{t_{134}} \rho_w(\bar{T}_k) C_p(\bar{T}_k)(\bar{T}_k - T_{ref})dt \tag{9}$$

and where the factor 4 takes into account the two symmetries of the simulation model. The results are summarized in Table 3 where the energies are given in Mega Joules. The energy recovered by extraction is $E = U_x - U_0 = 1.9757\ MJ$ which represents about 82% of the amount of energy stored. This is within the range 74,8% - 86,4% of the physical tests results on the mock-up and its theoretical model calculation as well as those for the real size ULISSE storage reservoir in a lake (2 Mm^3) [2].
The real energy balance must consider the energy used for pumping and the losses in the extraction tubes. Thus, the effective amount of energy available for usage would be less. However, the result shows the huge potential of the system to store energy. We also must bear in mind that the energy of the injected water is coming from the sun and is free of charge.

U_0	U_i	U_{64}	U_{70}
0.3861	7.8920	2.7891	2.4608
E_S	E_a	E_L	U_x
2.403	2.0747	0.3283	2.3618

***Table 3**: Energy balance results (MJ)*

Conclusions

This work shows the ability to use multiphysics simulation with Comsol Multiphysics to understand the behavior of the ULISSE system. Provided that the simulation model represents with enough accuracy the system, it would be possible to predict with a good approximation the energy balance. The model we did shows with a good agreement the evolution the system in the range of uncertainty and enhances the importance of the convection currents and diffusion in the energy loss. The consequence is the adaptation of the water extraction debt in order to minimize these losses.
The next steps of improvement of the multiphysics modelling would be to integrate in the model the fluid structure interaction. In a lake, the dynamics of the water is more complex, producing underwater mechanical waves [6], [7]. The integration of that dynamics in the Comsol Multiphysics model should help to understand the resistance of the ULISSE structure to such waves. The project should be continued by the construction of a bigger mock-up in conditions closer to the real operation and allowing to improve the numerical modelling.

References

[1] W. van Sprolant, Proposal for the CORSAIRE energy project as part of a sustainable development effort, EPS 10 Trends in Physics, 10th General Conference of the European Physical Society, September 9-13, 1996, Sevilla (Spain).

[2] W. van Sprolant, ULISSE, Under Lake Infrastructure for thermal capture and Storage of Solar Energy, OFEN Final Report, (2023).

[3] A. Gaudard, M. Schmid, A. Wüest, Utilisation thermique des eaux superficielles, potentiel des lacs et rivières suisses, Eawag et EPFL, AQUA & GAS N₀ 6., 2018.

[4] https://www.comsol.com/model/free-convection-in-a-water-glass-195.

[5] A. Benkhelifa, A. Bouhdjar, A. Harhad, Influence des forces d'inertie sur les performances de stockage thermique dans une cuve cylindrique durant les phases de charge et de décharge. Rev. Energ. Ren., Vol. 1 (1998), 53-63.

[6] Beito Fernandez Castro et al., Seasonality modulates wind-drive mixing pathways in a large lake, Communications Earth & Environment (2021) 2:215.

[7] Z. Vescernyes, Horizontal mixing dynamics in the upper layer of lake Geneva, 10.5075/epfl-thesis-943 (1991).

Acknowledgements

The authors wish to kindly thank the Swiss Federal Office of Energy (SFOE, Bern, Switzerland) for having supported this project.